Journal of Catalysis **195,** 298–303 (2000)
doi:10.1006/jcat.2000.2980, available online at http://www.idealibrary.com on IDEAL®

Kinetics and Mechanism of the N_2O Reduction by NH_3 on a Fe-Zeolite-Beta Catalyst

Bernard Coq,†,[1] Mathias Mauvezin,* Gérard Delahay,* and Stephane Kieger†

**Laboratoire de Matériaux Catalytiques et Catalyse en Chimie Organique, UMR CNRS-ENSCM 5618, ENSCM, 8 rue d'Ecole Normale, 34296 Montpellier Cedex 5, France; and †Grande Paroisse, 12 place de l'Iris, 92062, Paris-La Défense Cedex, France*

Received February 27, 2000; revised June 13, 2000; accepted June 21, 2000

In the context of decreasing the emissions of greenhouse gases, a Fe-exchanged zeolite-beta (Fe-BEA) catalyst is shown to be very active in the reduction of N_2O by NH_3 in the presence of O_2. The temperature at which 50% N_2O conversion is obtained is lower by ca. 80 K compared to its catalytic decomposition in the absence of NH_3. TPR, TPO, and TPD experiments after treatments in various atmospheres provide evidence that the reaction involves the redox cycle $Fe^{III} \leftrightarrow Fe^{II}$ where the Fe^{III} active species are Fe oxocations of low nuclearity. N_2O decomposes into O^* surface species on specific reduced Fe sites with the concurrent release of N_2; these species do not compete with O^* coming from O_2 for their removal by NH_3. In the absence of O_2, catalytic experiments with $^{14}N_2O$ and $^{15}NH_3$ show that: (1) N_2 is mainly formed from $^{14}N^{14}N$–O splitting to yield $^{14}N_2$, the O^* species being in turn removed by $^{15}NH_3$ to give $^{15}N_2$; (2) some ^{14}N–^{14}NO bond splitting occurs, which leads to $^{14}N^{15}N$ after reaction of $^{14}NO^*$ and $^{15}NH_3$ through a classical SCR mechanism. The Fe active species in the N–NO splitting are inhibited in the presence of O_2. The kinetics of N_2O reduction by NH_3 obeys a Mars and van Krevelen oxido–reduction mechanism modified with an inhibiting term of NH_3. © 2000 Academic Press

Key Words: **nitrous oxide; ammonia; Fe-zeolite; reduction; mechanism.**

INTRODUCTION

Nitrous oxide exhibits a high potential contribution to the greenhouse effect and takes part in the destruction of the stratospheric ozone layer. N_2O is included after CO_2 and CH_4 in the list of "greenhouse gases." At present, every year the N_2O concentration in the atmosphere is rising by 0.25%. The main causes for this increase are anthropogenic activities, such as agriculture and industrial and combustion processes, including emissions from road vehicles. Among industrial processes, the manufacture of adipic acid and nitric acid are the most important emitter of N_2O. At the Kyoto Conference in 1997, the EU committed itself to reduce by 8% in 2010 the emissions of greenhouse gases based on the values of 1990.

The simplest control technology for N_2O release is based on the catalytic decomposition to N_2 and O_2 (1), and Fe–zeolite catalysts are among the most active materials in the presence of O_2, though they remain not efficient enough. It was proposed that the decomposition of N_2O over Fe–zeolites is based on the redox cycle $Fe^{III} \leftrightarrow Fe^{II}$ with the desorption of adsorbed oxygen as the slow step (1). A boosting effect of reductant addition on the decomposition of N_2O was experimentally identified (1–10) and might be interpreted by a faster removal of surface oxygen. It was shown that Fe–ZSM-5 are efficient catalysts for the reduction of N_2O using propane or propene as reductants (4, 6, 10). However, the selectivity of hydrocarbon oxidation to CO was high (4). Moreover, when $NO + N_2O$ mixtures were processed there was a retardation of the onset of N_2O conversion to higher temperatures and the NO conversion levelled off at ca. 40–50% (4). In contrast, when $NO + N_2O$ mixtures were reduced by NH_3 on a Fe–zeolite-beta (Fe-BEA) catalyst, there was a synergistic effect on both the conversion of NO and N_2O which occurred at lower temperature than when processed alone (11); moreover, full NO conversion was reached rapidly. NH_3 is almost always the reductant used in the selective catalytic reduction (SCR) of $NO + NO_2$ mixture from off-gases of power plants and nitric acid plants (12, 13), in which N_2O is often also present. However, no fundamental study exists pertaining to the reduction of N_2O by NH_3 in presence of O_2. The aim of this work was to elucidate some aspects of the mechanism and the kinetics of this reaction on a Fe-BEA catalyst, in view of developing new active materials at low temperature for N_2O reduction.

EXPERIMENTAL

The Fe-BEA catalyst was prepared by ion exchange of 5 g of H-BEA (Zeolyst PQ Corp., specific surface area $\approx 680\ m^2g^{-1}$, Si/Al ≈ 12.5, grain size: 120–250 μm) with 100 cm^3 $Fe(NO_3)_3 \cdot 9H_2O$ at a pH of ≈ 4. After filtration, the solid was dried at 393 K in an oven and then calcined at 823 K in flowing air overnight (120 $cm^3\ min^{-1}$). The chemical analysis was performed at the Service Central d'Analyse

---

[1] To whom correspondence should be addressed. Fax: (+33) 4 67 14 43 49. E-mail: coq@cit.enscm.fr.

0021-9517/00 $35.00

du CNRS (Vernaison, France) by ICP. The amount of Fe (1.9 wt%) corresponds to a theoretical exchange degree of 97% (300Fe/Al). The nature and the amount of various Fe species were determined by Mössbauer spectroscopy (EG&G) and temperature-programmed reduction experiments by H_2/Ar (TPR). The TPR, TPO (temperature-programmed oxidation), and TPD (temperature-programmed desorption) of Fe-BEA activated in various conditions were carried out with a Micromeritics 2910 AutoChem apparatus at 10 K min^{-1}. The detection was performed with TCD and helped by mass spectroscopy coupling when necessary.

Before the catalytic tests, the sample ($\approx$200 mg) was reactivated *in situ* at 823 K in air in a quartz fixed-bed reactor (i.d.: 6 mm, depth of the catalytic bed). The decomposition of N_2O ($N_2O/O_2/He = 0.2/3/96.8$) and the SCR of N_2O ($N_2O/NH_3/O_2/He = 0.2/0.2/3/96.6$) were performed in the temperature-programmed surface reaction mode from 300 to 773 K (ramp: 10 K min^{-1}, space velocity: 35,000 h^{-1}). Experiments with $^{15}NH_3$ and kinetic studies were carried out at the steady state ($T = 618$ K) in the SCR of N_2O at various space velocities. In the kinetic studies the partial pressures of N_2O, NH_3, and O_2 in the feed were varied in the following ranges: $0 < P(N_2O) < 0.45$ kPa (4500 ppm), $0 < P(NH_3) < 0.4$ kPa (4000 ppm), and $0 < P(O_2) < 4$ kPa (4%). The conversion was then maintained at lower than 20% for using the reactor in the differential mode. The detection was performed with a quadrupole mass spectrometer BALZERS Omnistar and a Bruker Equinox 55 FTIR spectrometer. Nine masses characteristic of NO (30), NO_2 (30, 46), N_2O (28, 30, 44), $^{14}N_2$ (28), $^{15}N^{14}N$ (29), $^{15}N_2$ (30), NH_3 (17, 18), H_2O (17, 18), O_2 (16, 32), and He (4) were followed. When overlapping occurs in the same masses between several compounds, the contributions of each compound were determined by solving a linear system of equations. Calibrations were done on selected masses and wavelengths before and after each catalytic experiment.

RESULTS AND DISCUSSION

After calcination at 823 K in air, iron in Fe-BEA is distributed as ca. 2% Fe_2O_3 and 98% Fe-containing ions as shown by TPR (Fig. 1) and Mössbauer spectroscopy (doublet with isomer shift at 0.34 and quadrupole splitting at 1.1 mm s^{-1}, characteristic of Fe^{3+} in an octahedral environment). In a TPR experiment the choice of the reducing gas composition (H_2/Ar, 25/75) was done with respect to a balance between reduction of Fe species below 1300 K and sensitivity. In the TPR of Fe-BEA, the peak at 623 K corresponds to the reduction of Fe^{3+} to Fe^{2+} species and of Fe_2O_3 aggregates to Fe_3O_4. The latter species are then reduced to FeO and to Fe^0 clusters at 870 K. Fe^{2+} reduces to Fe^0 with collapse of the zeolite network above 1100–1200 K. The H_2 consumption below 800 K is H_2/Fe 0.42, which provides evidence that a part of the Fe species was still reduced or was unreducible in these conditions. The second proposal is preferred since Mössbauer spectroscopy has not shown any contribution of Fe^{II} species in the starting material. These findings are in good agreement with previous TPR studies on Fe- zeolite materials (14, 15).

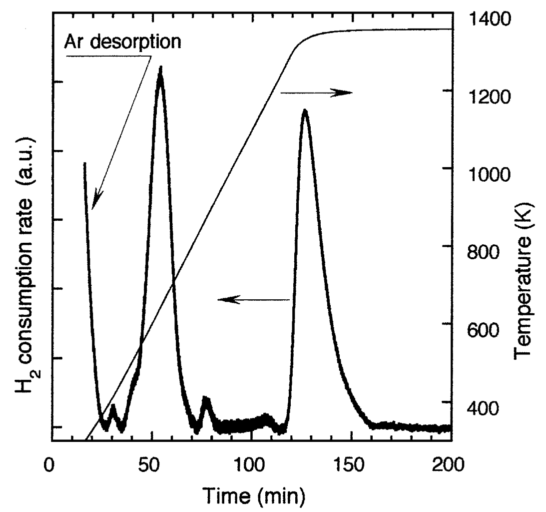

FIG. 1. TPR profile of the Fe-BEA. Conditions: H_2/Ar (25/75), ramp = 10 K min^{-1}.

The reduction of N_2O by NH_3 in the presence of O_2 on Fe-BEA starts at ca. 570 K and reaches 90% at ca. 650 K (Fig. 2). N_2 and H_2O were only detected as products. The onset of N_2O decomposition occurs at ca. 630 K to yield N_2 and O_2 (Fig. 2). The boosting effect of NH_3 on the N_2O reduction to N_2 is thus evidenced with a decrease of the light-off temperature (50% of N_2O conversion) by

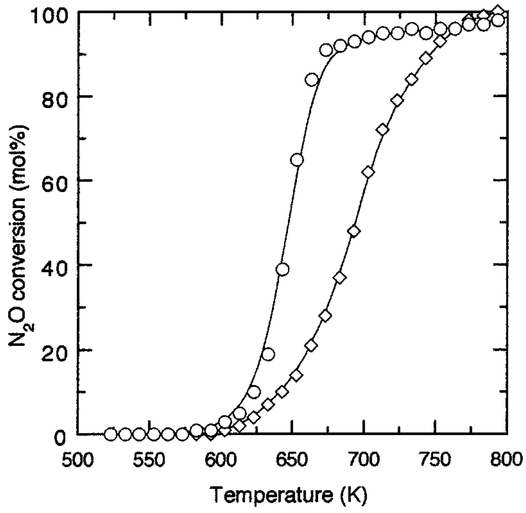

FIG. 2. SCR of N_2O by NH_3 (○) and N_2O decomposition (◇) as a function of temperature on Fe-BEA. Conditions: SCR of N_2O, $N_2O/NH_3/O_2/He = 0.2/0.2/3/99.6$; N_2O decomposition, $N_2O/O_2/He = 0.2/3/99.8$; ramp = 10 K min^{-1}, space velocity = 35,000 h^{-1}.

ca. 80 K compared to that of N_2O decomposition. We have previously reported that the promoting effect of NH_3 on N_2O reduction on Fe-zeolite depended on the nature of the zeolite (16). It was very low for Fe-FER, but the largest for Fe-BEA and Fe-MFI.

In its simplest form the catalytic decomposition of N_2O has been described by Eqs. [1]–[3] (1, 17):

$$N_2O + {}^* \rightarrow N_2 + O^* \qquad [1]$$

$$N_2O + O^* \rightarrow N_2 + O_2 + {}^* \qquad [2]$$

$$2O^* \leftrightarrow O_2 + 2^*. \qquad [3]$$

In the presence of NH_3, the surface oxygen can also be removed according to Eq. [4]:

$$2NH_3 + 3O^* \rightarrow N_2 + 3H_2O + 3^*. \qquad [4]$$

It should be pointed out that a possible small release of O_2, according to Eqs. [1] and [2], might not be identified in the SCR of N_2O by NH_3 due to the large excess of O_2. However, N_2O reduction by NH_3 in the absence of O_2 has not shown any formation of O_2 below 740 K, and the stoichiometry of the reaction was $N_2O/NH_3 \approx 3/2$. This is a strong argument that allows one to postulate that since no O_2 release occurred during the reduction of N_2O by NH_3 in the absence of O_2, this very likely remains true when O_2 is present in the feed. There is thus no interference between the SCR of N_2O by NH_3 and its catalytic decomposition below 620 K.

The influence of O_2 content on N_2O and NH_3 conversion rates was first studied by classical kinetics at 618 K and steady state; no deactivation was observed. The rate of N_2O reduction only increased very slightly with O_2 content (Fig. 3). The inhibition by O_2 of the N_2O reduction, when occurring, could be understood by Eq. [3] backward. This inhibition is generally low for Fe species exchanged in a zeolite matrix (1, 7), and this is confirmed for the present Fe-BEA catalyst. In contrast, O_2 accelerated sharply the oxidation of NH_3 to N_2, which reached a plateau above 2000 ppm O_2 (Fig. 3). This behavior likely means that NH_3 reacts with two different surface oxygens in Eq. [4], coming either from N_2O or from O_2. This can be correlated with the different TPD profiles from Fe-BEA calcined in O_2/N_2 (20/80) at 773 K (Fig. 4a) on the one hand and activated at 773 K in N_2O/He (5/95) after reduction at 773 K in H_2/Ar (25/75) on the other hand (Fig. 4b). One should be precise in that after activation at 773 K in N_2O/He the sample was cooled to room temperature in the same gas. After calcination in O_2/N_2, a broad peak of O_2 desorption with shoulders appears in the range 800–1100 K. After activation in N_2O/He of the reduced Fe-BEA, there is always a broad peak of O_2 desorption at high temperature (>800 K) but several other desorption peaks of large magnitude appeared at lower temperatures. The natures of desorbing species were identified by mass spectroscopy, which allowed one to attribute desorption peaks to N_2O at 450 K and to NO at ca. 660 K and three peaks of O_2 desorption at 610, 790, and 940 K. It clearly appears that a different surface

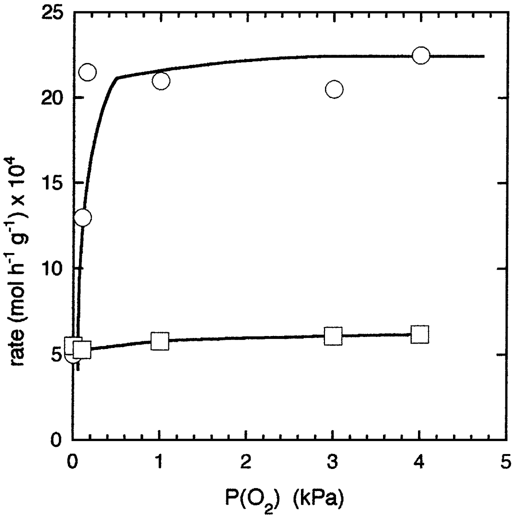

FIG. 3. Rates of N_2O reduction by NH_3 (□) and of NH_3 oxidation (○) as a function of $P(O_2)$ on Fe-BEA. Conditions: $T_R = 618$ K, space velocity = 25,000–35,000 h^{-1}, $P(N_2O) = P(NH_3) = 0.2$ kPa, balance with He.

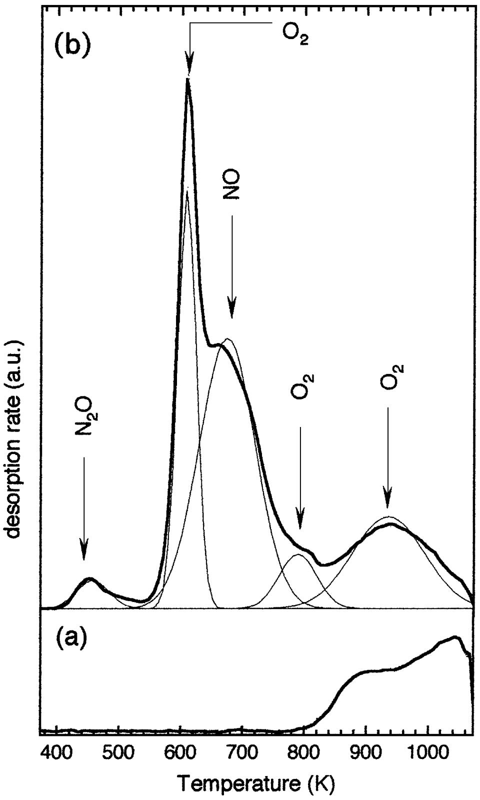

FIG. 4. (a) TPD from Fe-BEA calcined in O_2/N_2 (20/80) at 773 K. (b) TPD from Fe-BEA activated in N_2O/He (5/95) at 773 K after reduction in H_2/Ar (25/75) at 773 K. Conditions: ramp = 10 K min^{-1}.

oxygen exists after N_2O treatment, which desorbs in a significant amount at low temperature ($\approx$610 K). One may speculate that this surface oxygen is analogous to that proposed to be formed by interaction of N_2O with Fe-ZSM-5 zeolite and called α-oxygen (18). These species were proposed to be associated with binuclear Fe complexes rather than with isolated atoms (19).

In the reduction of N_2O by NH_3 we normally expected that the reaction was regulated by Eqs. [1] and [4] since O_2 formation was never detected. In a reaction of $^{14}N_2O$ with $^{15}NH_3$, the isotopic distribution of labelled dinitrogen isotopomers would therefore be 25% $^{15}N_2$ and 75% $^{14}N_2$. Since O_2 has little influence on the rate of N_2O reaction with NH_3, we first carried out the reduction of $^{14}N_2O$ by $^{15}NH_3$ in the absence of O_2 (618 K, steady state conditions, high N_2O conversion by tuning the space velocity). The distribution of N_2 isotopomers is shown in Fig. 5 as a function of time. Surprisingly, about 17% $^{14}N^{15}N$ was thus formed, which could not be taken into account by Eqs. [1] and [4]. However, when the same experiment was carried out in an O_2-rich atmosphere, the amount of $^{14}N^{15}N$ did not exceed 2% (Fig. 5). When the isotopomer was switched from $^{15}NH_3$ to $^{14}NH_3$, the proportion of $^{14}N^{15}N$ went through a maximum before decreasing to zero. This is a transient phenomenon due to substitution of adsorbed $^{15}NH_3$ by $^{14}NH_3$; $^{15}NH_3$ and $^{14}NH_3$, both present on the surface, then react according to Eq. [4] to yield $^{14}N^{15}N$.

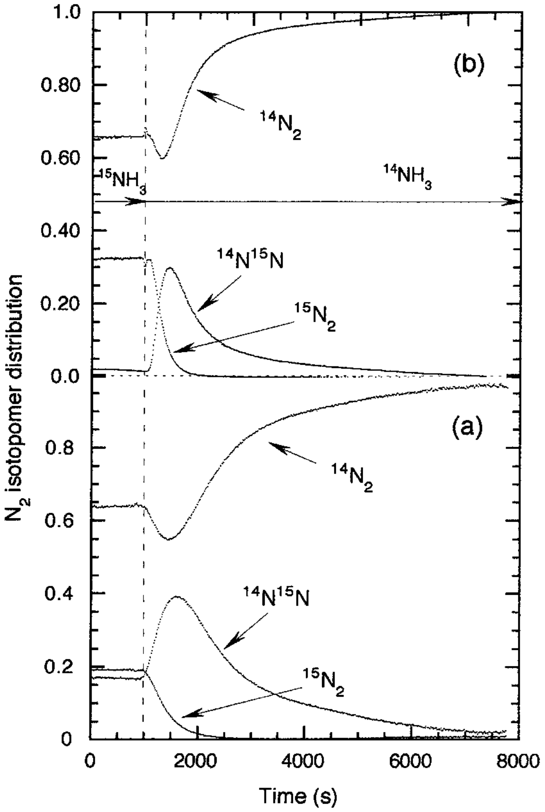

FIG. 5. Distribution of N_2 isotopomers in the reduction of $^{14}N_2O$, from 0 to 1000 s by $^{15}NH_3$ and then by $^{14}NH_3$, on Fe-BEA: (a) without O_2, (b) with 3% O_2. Conditions: $T_R = 618$ K, $P(N_2O) = P(NH_3) = 0.2$ kPa, space velocity $\approx$ 10,000 h^{-1}.

N–NO splitting would normally lead to NO and N_2. NO was not identified in the course of the reaction, but in the TPD from Fe-BEA after N_2O treatment (Fig. 4b), an NO desorption peak indeed appeared at 660 K. Moreover, we have shown that the SCR of NO in the presence of N_2O ($NO/N_2O < 1$) is extremely fast on Fe-BEA, even in the absence of O_2 (11). This could explain why NO has not been detected in the effluent during the catalytic experiments. These results suggest that a minor reaction, which may be described stoichiometrically as $2N_2O \rightarrow N_2 + 2NO$, may also occur by breaking of the much stronger N–NO bond (481 kJ mol^{-1}) rather than the weaker NN–O bond (167 kJ mol^{-1}). Such a reaction was evidenced recently in the decomposition of N_2O on Ba/MgO (20). The desorption of NO at ca. 610 K has also been identified in the TPD of Fe-ZSM-5 after exposure to N_2O at 473 K (21).

We can thus propose that the reduction of N_2O by NH_3 very likely proceeds according to a redox cycle of "Fe ions" involving N_2O and NH_3 as an oxidant and reductant interacting on separated sites with the splitting on the NN–O bond in N_2O. A minor contribution exists, coming from N–NO splitting and the subsequent SCR of NO by NH_3. The iron sites responsible for the N–NO bond splitting are inhibited in the presence of O_2.

Temperature-programmed reduction and oxidation experiments were carried out to obtain more insight into the redox mechanism. In these experiments, the nature of released gases was followed by mass spectroscopy detection. We wished first to carry out TPO by N_2O after activation of Fe-BEA in NH_3. Actually, NH_3 remained too strongly bonded on the catalyst and desorbed upto 1100 K (22). This behavior alters the results since the reaction $NH_3 + N_2O$ then superimposes to the oxidation of reduced Fe species by N_2O. However, additional experiments have shown that after reduction by NH_3/He (0.2/99.8) at 773 K of Fe-BEA, there was no more H_2 consumption when TPR was carried out up to 773 K in H_2/Ar (25/75). We have then concluded that the reduction state of the Fe species is very similar when Fe-BEA is activated at 773 K in NH_3/He (0.2/99.8) or H_2/Ar (25/75). TPO by N_2O/He (0.2/99.8) was therefore carried out after activation of Fe-BEA in H_2/Ar (25/75) at 773 K. The TPO profile (Fig. 6a) shows two waves of N_2O consumption:

(1) The first N_2O consumption occurs at medium temperatures (473–673 K), with the release of N_2 only, and corresponds to the specific interaction between N_2O and reduced Fe sites with the anchoring of O*. As compared to the total Fe content, N_2O consumption is $N_2O/Fe \approx 0.52$ (mol/mol). It is however important to keep in mind that

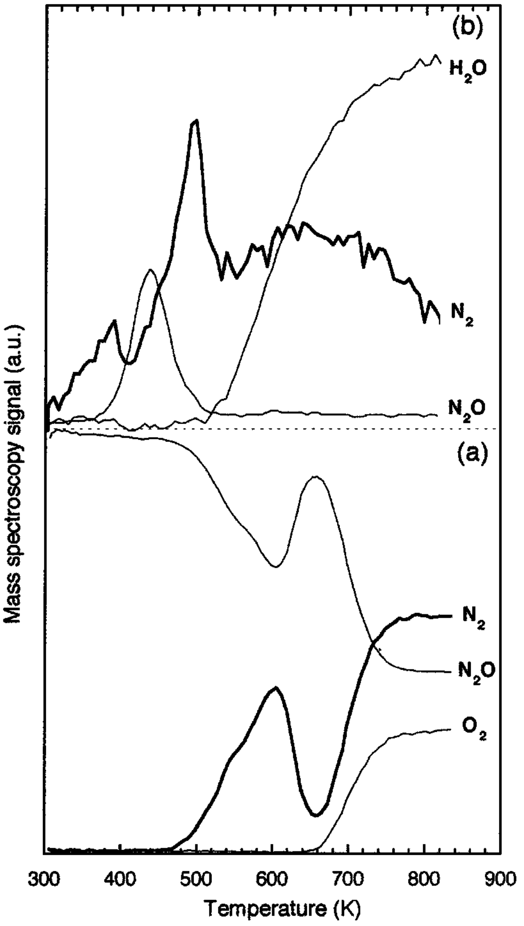

FIG. 6. (a) TPO by N_2O/He (0.2/99.8) of Fe-BEA after reduction in H_2/Ar (25/75) at 773 K. (b) TPR by NH_3/He (0.2/99.8) of Fe-BEA after oxidation in N_2O/He (0.2/99.8) at 773 K. Conditions: ramp = 10 K min^{-1}, space velocity = 10,000 h^{-1}, mass spectroscopy detection.

a part of the Fe^{3+} species was not reduced by treatment in H_2/Ar (25/75), as the TPR experiment showed (Fig. 1, *vide supra*); on that account, the actual consumption of N_2O per reduced "Fe site" is likely in the range 0.5–1.

(2) The onset of the second N_2O consumption starts around 650 K and corresponds to the initiation of the catalytic decomposition of N_2O into N_2 and O_2.

TPR by NH_3/He (0.2/99.8) has been carried out after oxidation by N_2O/He (0.2/99.8) at 773 K of Fe-BEA previously reduced (Fig. 6b). In the course of TPR, very strong adsorption of NH_3 made its concentration profile uninformative. In contrast, the release of N_2 formed is very clear and occurs as a broad peak with shoulders between 373 and 773 K. The expected H_2O released is delayed due to retention on the BEA zeolite. As compared to the total Fe content, the N_2 formation is $N_2/Fe \approx 0.20$ (mol/mol), which corresponds to an NH_3 consumption of $NH_3/Fe \approx 0.40$.

If one compares the two profiles of TPR by NH_3 and TPO by N_2O (Fig. 6), it is worth to noting that the onset of the TPR profile occurs at lower temperatures. One might speculate that in the oxido–reduction cycle of iron, which regulates the reaction $N_2O + NH_3$, the oxidation of the reduced Fe sites by N_2O would likely be the rate-determining step. Moreover, we can also notice that in the course of the TPO/TPR sequence the normalised N_2O/Fe and NH_3/Fe consumptions are in very good agreement with the stoichiometry $N_2O/NH_3 = 3/2$ of the global reaction $3N_2O + 2NH_3 \rightarrow 4N_2 + 3H_2O$.

In the very classical kinetic treatment of oxido–reduction reactions by Mars and van Krevelen (23), the rate law of the reaction $N_2O + NH_3$ will take the following form: $r = k_1P(N_2O)k_2P(NH_3)/[k_1P(N_2O + k_2P(NH_3)]$. The rate dependency as a function of N_2O content (Fig. 7) in the feed is in agreement with this kinetic law. In contrast, the evolution of the rate as a function of NH_3 content (Fig. 8) does not obey this kinetic law and goes through a maximum value for $P(NH_3) \approx 0.06$ kPa (600 ppm). Taking into account that NH_3 is strongly bonded on Fe-BEA (20), an inhibiting effect of NH_3 on the oxidation of reduced Fe sites can be considered. Since the precise nature of reduced and oxidized Fe sites could not be identified, in the following we will denote these sites as "Fe^{II}" and "Fe^{III}–O", respectively. The following reaction sequence can be proposed:

—reduction of N_2O: $$N_2O + \text{“}Fe^{II}\text{”} \xrightarrow{k_1} N_2 + \text{“}Fe^{III} - O\text{”} \qquad [5]$$

—oxidation of NH_3: $$2/3NH_3 + \text{“}Fe^{III} - O\text{”} \xrightarrow{k_2} 1/3N_2 + \text{“}Fe^{II}\text{”} + H_2O \qquad [6]$$

—adsorption of NH_3: $$\text{“}Fe^{II}\text{”} + \alpha NH_3 \xleftrightarrow{\lambda_1} \text{“}Fe^{II}\text{”}\,(NH_3)_\alpha. \qquad [7]$$

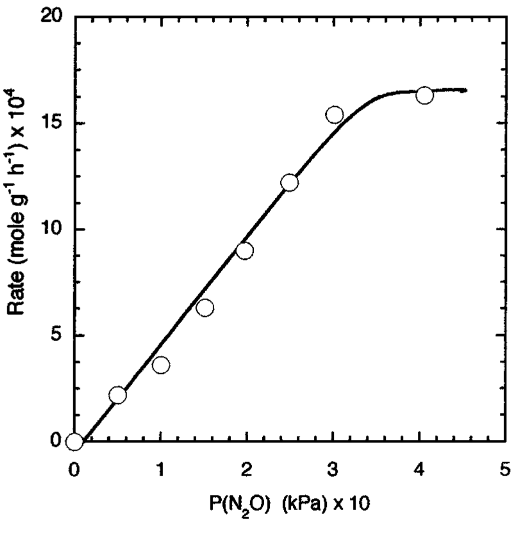

FIG. 7. Rate of N_2O reduction by NH_3 on Fe-BEA as a function of P(N_2O). Conditions: $T_R = 618$ K, space velocity = 25,000–35,000 h^{-1}, $P(NH_3) = 0.2$ kPa, $P(O_2) = 3$ kPa, balance with He.

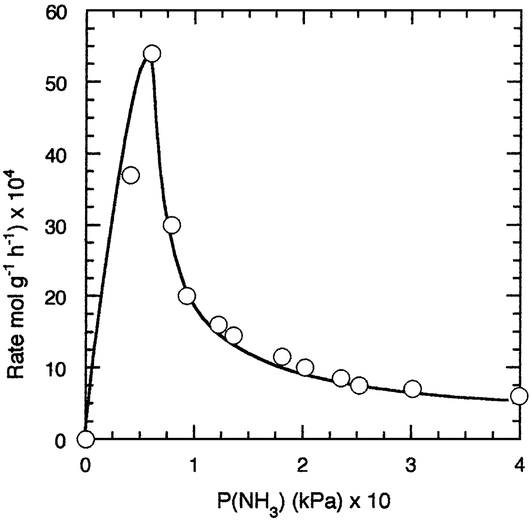

FIG. 8. Rate of N_2O reduction by NH_3 on Fe-BEA as a function of $P(NH_3)$. Conditions: $T_R = 618$ K, space velocity = 10,000–50,000 h^{-1}, $P(N_2O) = 0.2$ kPa, $P(O_2) = 3$ kPa, balance with He.

This is a very simplified approach that is only aimed at demonstrating that an inhibiting term in NH_3 can account for a volcano-shaped dependency of the rate versus NH_3 pressure. Assuming that the "Fe^{II}"$(NH_3)_\alpha$ species exhibit very low reactivity to be reoxidized by N_2O directly, compared to "Fe^{II}", the following rate expression can be derived from a classical kinetic treatment:

$$r = \frac{k_1 P_{N_2O} k_2 P_{NH_3}^{2/3}}{k_1 P_{N_2O} + k_2 \left[1 + \lambda_1 P_{NH_3}^{\alpha}\right] P_{NH_3}^{2/3}}. \quad [8]$$

One can see that the partial order with respect to N_2O varies from 1 to 0 when the N_2O pressure increases, in agreement with data from Fig. 7. Moreover, Eq. [8] indeed accounts for the volcano-shaped dependency of the rate with the NH_3 pressure. However, the determination of rate and adsorption constants as well as the α exponant would need a much more detailed and dedicated kinetic study, which has not yet been undertaken.

CONCLUSION

The present study has demonstrated that NH_3 accelerates the reduction of N_2O to N_2 on Fe-BEA. In the presence of O_2 we propose that N_2O conversion occurs through the redox cycle $Fe^{III} \leftrightarrow Fe^{II}$ with NN–O splitting mainly. N_2O oxidizes Fe^{II} to lead Fe^{III}-oxocations, which are regenerated back to Fe^{II} by NH_3. However, significant N–NO splitting occurs in the absence of O_2. There is no inhibiting effect of O_2 for the reduction of N_2O by NH_3, which obeys a modified Mars and van Krevelen oxido–reduction kinetics, taking into account an inhibiting term of NH_3.

ACKNOWLEDGMENT

M.M. warmly thanks the "Ministère Français de l'Education Nationale, de la Recherche et de la Technologie" for a scholarship.

REFERENCES

1. Kapteijn, F., Rodriguez-Mirasol, J., and Moulijn, J. A., *Appl. Catal. B* **9**, 25 (1996).
2. Petunchi, J. O., and Hall, W. K., *J. Catal.* **78**, 327 (1982).
3. Kato, Y., Konishi, K., and Ohta, M., U.S. Patent 4 571 329 (1986), to Babcock-Hitachi Kabushiki Kaisha.
4. (a) Kögel, M., Mönnig, R., Schwieger, W., Tissler, A., and Turek, T., *J. Catal.* **182**, 470 (1999). (b) Kögel, M., Sandoval, V. H., Schwieger, W., Tissler, A., and Turek, T., *Catal. Lett.* **51**, 23 (1998).
5. Randall, H., Doepper, R., and Renken, A., *Appl. Catal. B* **17**, 357 (1998).
6. Pophal, C., Yogo, T., Yamada, K., and Segawa, K., *Appl. Catal. B* **16**, 177 (1998).
7. Mauvezin, M., Delahay, G., Coq, B., and Kieger, S., *Appl. Catal. B* **23**, L79 (1999).
8. Delahay, G., Mauvezin, M., Coq, B., and Neveu, B., French Pat. demand 99.0.1999 to Grande Paroisse ATO.
9. Kapteijn, F., Rodriguez-Mirasol, J., Mul, G., Marbán, G., and Moulijn, J. A., "Proceedings, 11th International Congress on Catalysis, Baltimore, 1996" (J. W. Hightower W. N. Delgass, E. Iglesia, and A. T. Bell, Eds.), p. 641. Elsevier, Amsterdam 1996.
10. Centi, G., and Vazzana, F., *Catal. Today* **53**, 683 (1999).
11. Coq, B., Mauvezin, M., Delahay, G., Butet, J.-B., and Kieger, S., *Appl. Catal. B* **27**, 193 (2000).
12. Bosch, H., and Janssen, F., *Catal. Today* **2**, 369 (1987).
13. Forzatti, P., and Lietti, L., *Heterogeneous Chem. Rev.* **3**, 33 (1996).
14. Fang, S.-M., Petunchi, J., Leglise, J., Millman, W., and Hall, W. K., *J. Catal.* **96**, 182 (1985).
15. Chen, H.-Y., and Sachtler, W. M. H., *Catal. Today* **42**, 73 (1998).
16. Mauvezin, M., Delahay, G., Kißlich, F., Coq, B., and Kieger, S., *Catal. Lett.* **62**, 41 (1999).
17. Fu, C. M., Korchak, V. N., and Hall, W. H., *J. Catal.* **68**, 166 (1981).
18. Panov, G. I., Kharitonov, A., and Sobolev, V. I., *Appl. Catal.* **98**, 1 (1993).
19. Panov, G. I., Sobolev, V. I., Dubkov, K. A., Parmon, V. N., Ovanesyan, N. S., Shilov, A. E., and Shteinman, A. A., *React. Kinet. Catal. Lett.* **61**, 251 (1997).
20. Xie, S., and Lunsford, J. H., *Appl. Catal. A* **188**, 137 (1999).
21. El-Malki, E. M., van Santen, R. A., and Sachtler, W. M. H., *Microporous Mesoporous Mater.* **35–36**, 235 (2000).
22. Mauvezin, M., Delahay, G., and Coq, B., unpublished data.
23. Mars, P., and van Krevelen, D. W., *Chem. Eng. Sci.* **3**, 41 (1954).